Zero-Guard OFDM Performance in SFN with ATSC 3.0 Ultra-Robust Transmission Modes

Jose Luis Carcel, Jordi Joan Gimenez and David Gomez-Barquero
iTEAM Research Institute, Universitat Politecnica de Valencia
Valencia, Spain
Email: {jocarcer,jorgigan,dagobar}@iteam.upv.es

***Abstract*—Single Frequency Network (SFN) deployments are widely extended in DTT (Digital Terrestrial Television) to deliver the same signal across multiple transmitters. A large-enough guard interval (GI), or cyclic prefix (CP), is required to extend coverage area without SFN self-interference at the expense of increasing capacity overheads. The new DTT standard ATSC 3.0 offers unprecedented features and flexibility for ultra-robust transmissions with Carrier-to-Noise ratios (CNRs) well-below 0 dB. Such robust modes may cope with degradation caused by SFN self-interference, what could enable the suppression of the GI and a corresponding efficiency increase. This paper studies the performance of ultra-robust transmission modes of ATSC 3.0 without GI in SFNs. A set of these modes are compared in SFN scenarios, characterized by different path delays. The impact of the GI duration, scattered pilot (SP) patterns and associated pilot boosting (PB), as well as channel estimation algorithms are analyzed. The results show the potential of Zero-Guard OFDM operation with very low rates (e.g. QPSK 2/15, 3/15) compared to CP-OFDM, where the benefits in performance do not compensate the overhead penalties.**

***Index Terms*—Guard interval (GI); cyclic prefix (CP); ultra-robust code rates; ATSC 3.0; Single Frequency Network (SFN)**

I. Introduction

Single Frequency Networks (SFNs) are popular in DTT (Digital Terrestrial Television) technology to provide large area coverage by transmitting the same signals using the same frequencies across multiple stations in a synchronized fashion (generally by means of a GPS signal). The received signal in an SFN presents multiple echoes that may degrade performance due to Inter-Symbol Interference. The insertion of a large enough Guard Interval (GI), also known as Cyclic Prefix (CP), covering the maximum echo delay in the network enables the non-destructive contribution of signals. Figure 1 presents an illustrative example of a two-transmitter SFN with two signal paths. The GI duration is usually set up to cover the maximum distance between transmitters. The DVB-T2 (Digital Video Broadcasting Terrestrial 2^{nd} Generation) [1] as well as the new ATSC 3.0 (Advanced Television Systems Committee) [2] standards allow for large inter-site distances covering dozens to hundreds of kilometers (e.g. 60 km - GI duration of 200 μs - or 120 km - GI duration of 400 μs).

The configuration of ultra-robust transmission modes with Carrier-to-Noise threshold, C/N$_{min}$, well-below 0 dB, would allow for error-free reception even when noise is above signal power. This may counteract the effects of degradation due to Inter-Symbol Interference (ISI) in an SFN [3]. Recent studies have also considered the use of ultra-robust modulation and code rate (MODCOD) to withstand co-channel interference in networks with tight frequency reuse (see e.g. Cloud Transmission [4] and wideband DTT WiB [5]).

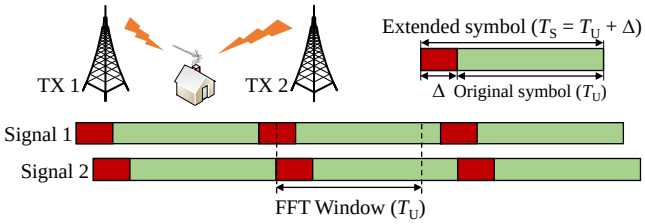

Fig. 1. SFN with 2 transmitters. Construction of the signal by appending the GI (Δ) as a prefix to the useful symbol.

ATSC 3.0 supports Low-Density Parity Check (LDPC) forward error correction (FEC) codes with twelve code rates (from 2/15 up to 13/15) and six modulation orders, from QPSK to 4k-NUC (Non-Uniform Constellation) [6]. The combination of the lowest modulation QPSK with very low code rates offers very robust operation.

The reduction (or elimination) of the GI would permit increasing capacity if the performance loss results low. On the other hand, the extra capacity could enable transmitting a more robust mode (e.g. a more robust MODCOD) while keeping the same total capacity.

This paper evaluates the bit error rate (BER) performance and feasibility of Zero-Guard OFDM compared to existing CP-OFDM systems in the context of SFN. The study considers the parameters that have a direct impact on the system performance in an SFN such as the pilot pattern as well as the channel estimation algorithm implemented at the receiver. Note that the GI is also used for symbol synchronization purposes [7], but this aspect is out of the scope of the paper.

The paper is structured in five sections. The first one introduces the key configuration parameters in ATSC 3.0 for CP-OFDM operation in SFN. The second section presents the methodology for performance evaluation using an ATSC 3.0 physical layer simulator. Next, performance results are presented for multiple transmission parameters. Finally, conclusions and network recommendations are presented.

To be presented at IEEE BMSB 2017

TABLE I
ALLOWED COMBINATIONS OF FFT SIZE, PP AND GI IN ATSC 3.0

Δ (μs)	d_{tx} (km)	FFT Size			Samples	O(%)
		8k	16k	32k		
27.87	8	✓	✓	✓	192	0.59
55.56	16	✓	✓	✓	384	1.17
74.07	22	✓	✓	✓	512	1.56
111.11	33	✓	✓	✓	768	2.34
148.15	44	✓	✓	✓	1024	3.12
222.22	66	✓	✓	✓	1536	4.68
296.30	88	✓	✓	✓	2048	6.25
351.85	105	✓	✓	✓	2432	7.42
444.4	133	N/A	✓	✓	3072	9.38
527.78	158	N/A	✓	✓	3648	11.13
592.59	178	N/A	✓	✓	4096	12.50
703.70	211	N/A	N/A	✓	4864	14.84

II. CP-OFDM OPERATION IN SFN

Correct operation of CP-OFDM against SFN echoes strongly depends on the selection of certain transmission parameters as well as operations conducted at the receiver. The most important parameters identified are the GI length as well as the scattered pilot (SP) pattern and corresponding pilot boosting (PB). At the receiver, the selection of a proper channel estimation algorithm that can deal with echoes is critical. Moreover, the GI is commonly used to allow for time synchronization. However this paper does not cover this aspect.

A. GI insertion in OFDM systems

A GI (Δ) is appended as a prefix to the original symbol T_U (useful symbol length), leading to a new symbol of length T_S (total symbol length), see Figure 1. In practice, the length of the GI needs to be greater than, or equal to, the maximum expected delay between signals to prevent performance loss caused by ISI. The duration of the FFT window remains as T_U, so that it can be positioned avoiding overlaps between consecutive symbols [8].

The length of the GI introduces a capacity overhead $\frac{\Delta}{T_U+\Delta}$. Table I shows the 12 different GI values available in ATSC 3.0. When expressed as a fraction of T_U, the maximum allowed delayed (Δ) and the maximum distance between transmitters so that echoes fall within the GI (d_{tx}), can be calculated[1]. Note that ATSC 3.0 does not allow certain combinations of GI and FFT size due to excessive overhead. The last column shows the capacity overhead in a 6 MHz channel with 32k FFT.

According to the selected GI duration, system performance generally depends on the power level of the received echoes and the relative delay between the different paths. Outside the GI, ISI degradation increases until a certain value, T_p, is reached. T_p is defined as the Nyquist limit and it is directly related to the chosen SP pattern and the ability of the channel estimation algorithm to resolve echoes in an SFN channel [9]. The calculation of T_p is addressed in the next sub-section.

[1] Δ and d_{tx} in Table I correspond to 32k FFT

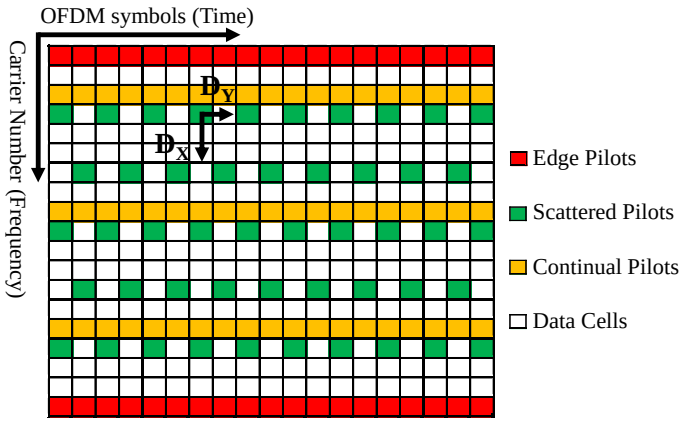

Fig. 2. Basic scheme of the type of pilots inserted in a frame in ATSC 3.0.

B. Channel Estimation in SFNs

1) Scattered Pilot Pattern selection: Figure 2 shows a basic scheme of the pilot patterns used per frame in ATSC 3.0. Scattered Pilots (SP) are employed for channel estimation. The parameters D_X (3, 4, 6, 8, 12, 16, 24, and 32) and D_Y (2 and 4) set the frequency separation between pilot-bearing carriers and the length of the SP in OFDM symbols, respectively [10]. Denser SPs (low D_X and/or D_Y) improve the channel estimation at the expense of an increased overhead. Better channel estimates can be also achieved by using pilot boosting (PB0 to PB4 in ATSC 3.0).

In an SFN, where echoes generate severe fading, the selection of a proper D_X is critical and has a direct influence in the value of the Nyquist limit T_p. When both frequency and time interpolation are implemented, the Nyquist limit gets the value $T_p = \frac{T_U}{D_X}$. T_p increasies when the useful symbol duration becomes larger (i.e. for larger FFT sizes) and in general for dense SP patterns since a more accurate channel estimation can be performed in the frequency domain.

2) Channel Estimation Algorithms: Channel estimation in OFDM systems is a two dimensional (2D) process that varies with time and frequency. The first step is to estimate the channel at the SP positions. A simple way of estimation is the Least Square (LS) estimation assuming two 1D processes. The LS estimation of the channel response $H_i[m]$ is obtained as:

$$\widehat{H}_i[m] = \frac{Y_i[m]}{X_i[m]} = H_i[m] + \frac{N_i[m] + \delta_{i_{ISI+ICI}}[m]}{X_i[m]} \quad (1)$$

where i is the OFDM symbol and m is the index of the sub-carrier, $X_i[m]$ is the transmitted signal, $N_i[m]$ is the AWGN noise and $\delta_{i_{ISI+ICI}}[m]$ express additional degradation due to ISI and ICI when the echoes are received outside the GI. An additional error may be introduced by non-ideal estimation.

TABLE II
SIMULATION PARAMETERS

Parameter	*Value*
LDPC FEC Size	64800 bits
Code Rate	2/15, 3/15, 4/15, 5/15, 10/15, 11/15
Modulation	QPSK
Bandwidth	6 MHz
FFT Size	32k
GI	1/16, 1/8
Scattered Pilot Pattern	SP3_2, SP6_2, SP12_2
Nyquist limit (T_p) (μs)	1580 (SP3_2), 790 (SP6_2), 395 (SP12_2)
Pilot Boosting	PB0, PB1, PB2, PB3, PB4
Channel Estimation (time)	Linear
Channel Estimation (freq)	Linear, DFT and DFT sub-window
Bit Error Rate target	10^{-4}
Channel Model	SFN channel defined in [12]
SFN Power Imbalance (dB)	0, -3, -6
SFN Path Delay (μs)	50, 100, 150, 200, 250, 300

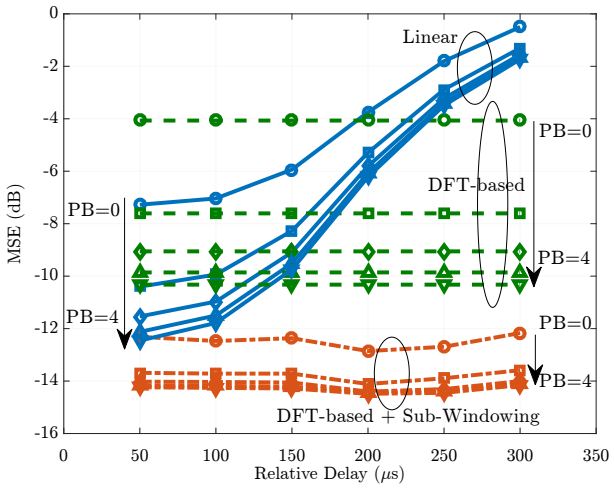

Fig. 3. MSE comparison in a 0 dB echo channel for channel estimation methods: linear, DFT-based and DFT-based with sub-windowing, for different pilot boosting (PB) values.

The second step is to extend the channel estimation at SP positions to the whole frame and data sub-carriers via interpolation. Depending on the interpolation method, the estimation accuracy and the interpolation error changes. In this paper, three methods are studied for frequency-domain interpolation:

a) Linear Interpolation: is a straightforward method in which the channel subcarriers are obtained by the result of a linear interpolation between the LS estimates. The method is well suited for smooth frequency variations but lacks of accuracy for severe fading in SFN, as results will show.

b) DFT-based interpolation: DFT-based interpolation [11] is performed by first calculating the IDFT of the LS estimates of the plot sub-carriers ($\widehat{H}_{SP}$). This operation provides the impulse response of the channel $\widehat{h}_{SP}$. In an SFN, the impulse response should present zero values beyond the last contribution (echo). The final interpolated channel is obtained by calculating the DFT.

c) DFT-based interpolation with sub-windowing: An enhanced method to increase the accuracy of the channel estimation is the DFT-based interpolation with sub-windowing, as described in [11]. In order to reduce estimation noise, $\widehat{h}_{SP}$ is divided into L narrow sub-windows. Those sub-bands that do not contain echo samples will be set to zero so that noise can be filtered.

III. Methodology for CP-OFDM and Zero-Guard OFDM Performance Evaluation

The performance of ultra-robust MODCODs in SFNs have been conducted by means of physical layer simulations using an ATSC 3.0 simulator developed and cross-checked during the standardization process. The configurations adopted for performance evaluation are listed in Table II.

The simulator has been adapted to the requirements of SFN simulations such as accurate noise and channel estimation processes:

- The SFN channel model is the 'simple two path profile, 0 dB Echo' described in [12] but extended to cover other power imbalances and echo delays.
- Noise plus ISI power has been estimated by calculating the difference between the average power of the continual pilots (see Figure 2) in all OFDM symbols, and their transmitted power as specified in the standard.
- Noise power estimation is obtained at the non-active carriers (at both edges) of the received OFDM signal spectrum.
- Regarding channel estimation, linear interpolation for time domain and linear, DFT-based and DFT-based with subwindowing (with $L = 256$) have been considered in the frequency domain.

IV. Results

This section presents the results of the study according to the methodology explained above, showing the performance of ultra-robust transmission modes in SFNs as well as the influence of channel estimation, SP pattern, pilot boosting, MODCOD and GI length.

A. Analysis of Channel Estimation Algorithms in SFN

A first study evaluates the MSE considering transmissions in a 0 dB echo channel with different channel estimation methods, QPSK modulation, coding rate 2/15 and different combinations of GI lengths, SP patterns and pilot boosting values into different CNR scenarios.

Figure 3 shows a comparison of MSE values for linear, DFT-based and DFT-based with sub-windowing, and for PB0 up to PB4. The computation is performed at CNR equal to 0 dB, GI 1/16 (296.3 μs with 32k FFT and 6 MHz BW) and SP12_2.

DFT with and without sub-windowing provide constant MSE for all the relative delays of the echo, while linear gets

worse with the increase of the delay. Moreover, DFT with sub-windowing shows better performance than linear and DFT as a consequence of the noise filtering, which introduces a gain from 4 up to 8 dB in MSE. For short relative delays linear performs better than the DFT method, mainly as a consequence of the noise effect of the latter case. For delays larger than 100-150 μs, linear gets a worse channel estimation than DFT as a result of the low density of the SP12_2. With respect to pilot boosting, only the change from PB0 to PB1 provides substantial improvement on the MSE. In terms of CNR, for DFT with sub-windowing PB1 introduces an improvement of 0.7 dB for SP12_2 and 0.1 dB for SP6_2 compared to PB0. For the linear and simple DFT cases, PB1 provides an improvement of 1.2 dB in the CNR performance for SP12_2 and 0.3 dB for SP6_2.

Larger GI, 1/8 (593 μs), has been studied with a denser pilot pattern, SP3_2 and harsh CNR conditions, -3 dB. Now, MSE values become constant for linear estimation along the delays due to the use of a denser SP. MSE performance is not improved by increasing the PB because of the high pilot density of SP3_2, where it degrades the CNR performance because of the data power reduction. For SP6_2, same performance as GI 1/16 is obtained, with PB1 improving 0.1 dB for DFT with sub-windowing and 0.3 dB for linear and simple DFT estimation. As a consequence, next results will assume a pilot boosting level depending on the density of the pattern (SP 3_2 will use PB0 and SP6_2 and SP12_2 will be used with PB1).

B. Performance Evaluation with Null-GI OFDM

Some CNR performance simulations are evaluated in this section in order to consider the influence of the GI absence while using robust code rates with QPSK. The required CNR has been obtained as a function of the relative delay between received signals, considering an SFN channel with different power imbalances. Some parameters have been fixed as SP12_2, PB1 and PB0, DFT with sub-windowing estimation. Two possible GI durations have been considered: GI 1/16, which is equivalent to a distance of 90 km between transmitters, and GI 1/8, corresponding to 180 km.

Figure 4 shows the influence of the different coding rates with QPSK. As it can be seen, low CRs as 2/15, 3/15, 4/15 or 5/15 are able to reduce the degradation introduced by the GI absence, showing values of degradation around 0.1 or 0.2 dB approximately. However, for higher CRs as 10/15 or 11/15 the effect of the ISI is quite remarkable, following an increasing tendency proportional to the CR level and the relative delay. Regarding the pilot pattern, if it is changed to SP6_2, slight improvements in performance are obtained as a result of the SP density increase.

On the other hand, if the GI is increased to 1/8, it is demonstrated that Zero-Guard operation is not efficient for any SP due to the ISI effect in longer echo relative delays. In this case, degradation for GI edge delay (600 μs) is about 1 dB for QPSK 3/15 or QPSK 4/15.

Note that degradation values have been obtained at GI edge. However, if delays at a certain distance from the edge are considered, performance loss becomes lower. As an example, for QPSK 4/15 the degradation is about 0.3 dB if the delay is considered at 75% of the GI edge.

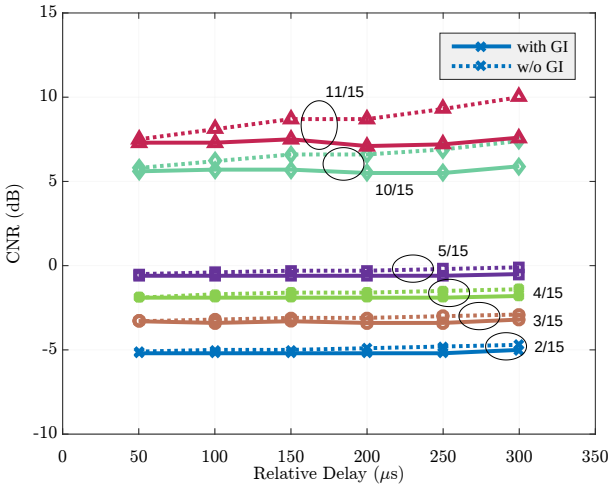

Fig. 4. Influence of code rate in CNR performance for QPSK with and without GI in 0 dB echo channel.

TABLE III
CNR DEGRADATION FOR SFN CHANNEL WITH DIFFERENT POWER IMBALANCES. GI 1/16 AND SP12_2

MODCOD	**0 dB echo**	**3 dB echo**	**6 dB echo**
QSPK 2/15	0.3 dB	0.1 dB	0 dB
QSPK 3/15	0.3 dB	0.2 dB	0.1 dB
QSPK 4/15	0.4 dB	0.2 dB	0.1 dB
QSPK 5/15	0.4 dB	0.1 dB	0.1 dB

Degradation due to GI absence can be lower if the echo power is considered 3 or 6 dB below the power of the main path, as shown in Table III. Assuming the previous parameters configuration with a 3 dB echo channel, the degradation is reduced to 0.1-0.2 dB for QPSK 2/15 or QPSK 3/15. If a lower power of the echo is considered, i.e. 6 dB echo channel, degradation becomes even lower, with values about 0-0.1 dB.

C. Overhead and Capacity evaluation

In this section a capacity evaluation is done with the aim of selecting which non-GI cases are efficient for real transmissions. Those cases resulting in degradation below 0.4 dB are studied (GI 1/16 for SP6_2 and SP12_2).

GI 1/16 introduces a 6.25% overhead and SP12_2 and SP6_2 a redundancy of about 4.17% and 8.33% respectively. CRs like 2/15 imply an 86.66% of redundancy, 3/15 an 80%, 4/15 a 73.33% and 5/15 a 66.66%. Taking into account these values and considering an effective bandwidth of 5.832 MHz, the resultant bitrate can be compared for the GI and non-GI cases as it is showed in Figure 5.

As it can be seen, some non-GI cases are equivalent in required CNR and bitrate to GI cases for a 3 dB echo channel. The degradation due to GI absence is about 0.2

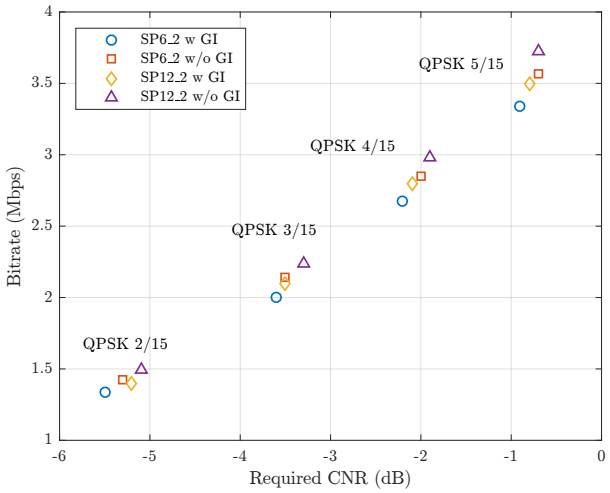

Fig. 5. CNR degradation vs Bitrate performance for QPSK and different pilot patterns in a 3 dB echo channel.

dB and the bitrate improvement is around 6.66%. For cases with lower echo relative power, e.g. 6 dB echo channel, degradation values become even lower, i.e. 0-0.1 dB for all the considered MODCODs. In this way, for the evaluated MODCODs Zero-Guard transmissions can be considered as a way of transmitting more information while keeping the same operation range.

V. Conclusions

The results discussed in this paper confirm the feasibility of supressing the GI (Guard Interval), or CP (Cyclic Prefix), in SFN scenarios. The use of ultra-robust transmission modes with CNR below 0 dB (e.g. QPSK 2/15 and 3/15) provides resilience against ISI that may allow reducing GI overheads. The performance of Zero-Guard OFDM has been shown for different scattered pilot patterns, signal path delays in an SFN, and considering a channel estimation method based on a DFT technique with noise filtering. Note that larger performance loss may be obtained with other frequency domain interpolation methods. SFN channel models with power imbalance 0 dB, 3 dB, and 6 dB echo have been evaluated. The study has considered that the GI is not overdimensioned, thus the evaluation has been conducted at the GI edge. If maximum echo delays are located at a certain fraction of the GI edge (e.g. at 50% or 75%) degradation values can be further reduced. For 0 dB echo, the minimum performance degradation of the CNR threshold is 0.3 dB, what makes the suppresion of the GI not attractive. With lower echo power, i.e. 3 dB and 6 dB, the elimination of the GI leads to very low performance loss (0.2 dB and 0.1 dB, respectively). In practice, such negligible degradation may enable the elimination of the GI, thus reducing overheads. This extra capacity may be translated into an increased bit rate (for the same coverage area) or an increased robustness keeping the capacity.

As future work, synchronization aspects in the absence of a GI should be analyzed since incorrect synchronization may generate critical performance loss. The performance of synchronization algorithms not directly linked to the presence of a GI should be carefully evaluated in order to allow Zero-Guard OFDM operation.

Acknowledgments

This work was supported in part by the European Commission under the 5G-PPP project 5G-Xcast (H2020-ICT-2016-2 call, grant number 761498). The views expressed in this contribution are those of the authors and do not necessarily represent the project. This work was also partially supported by the Ministerio de Educación y Ciencia, Spain (TEC2014-56483-R), co-funded by European FEDER funds.

References

[1] I. Eizmendi *et al.*, "DVB-T2: The Second Generation of Terrestrial Digital Video Broadcasting System," *IEEE Transactions on Broadcasting*, vol. 60, no. 2, pp. 258–271, June 2014.

[2] L. Fay, L. Michael, D. Gomez-Barquero, N. Ammar, and M. W. Caldwell, "An Overview of the ATSC 3.0 Physical Layer Specification," *IEEE Transactions on Broadcasting*, vol. 62, no. 1, pp. 159–171, March 2016.

[3] "SFN Frequency Planning and Network Implementation with regard to T-DAB and DVB-T," EBU, Tech. Rep. 024, Oct 2013.

[4] Y. Wu, B. Rong, K. Salehian, and G. Gagnon, "Cloud Transmission: A New Spectrum-Reuse Friendly Digital Terrestrial Broadcasting Transmission System," *IEEE Transactions on Broadcasting*, vol. 58, no. 3, pp. 329–337, Sept. 2012.

[5] E. Stare, J. Gimenez, and P. Klenner, "WIB: a new system concept for digital terrestrial television (DTT)," *The Best of IET and IBC 2016-2017*, vol. 8, pp. 4–9, 2016.

[6] L. Michael and D. Gomez-Barquero, "Bit-Interleaved Coded Modulation (BICM) for ATSC 3.0," *IEEE Transactions on Broadcasting*, vol. 62, no. 1, pp. 181–188, March 2016.

[7] W. L. Chin, "Blind Symbol Synchronization for OFDM Systems Using Cyclic Prefix in Time-Variant and Long-Echo Fading Channels," *IEEE Transactions on Vehicular Technology*, vol. 61, no. 1, pp. 185–195, Jan. 2012.

[8] R. Brugger and D. Hemingway, "OFDM Receivers. Impact on Coverage of Inter-Symbol Interference and FFT Window Positioning," EBU, Tech. Rep. Jul., 2003.

[9] "Frequency and Network Planning Aspects of DVB-T2," European Broadcasting Union, Tech. Rep. 3384, Nov 2013.

[10] E. Garro, J. J. Gimenez, S. I. Park, and D. Gomez-Barquero, "Scattered Pilot Performance and Optimization for ATSC 3.0," *IEEE Transactions on Broadcasting*, vol. 63, no. 1, pp. 282–292, March 2017.

[11] L. Zhang, Y. Wu, W. Li, Z. Hong, K. Salehian, H. M. Kim, S. I. Park, J. Y. Lee, P. Angueira, J. Montalban, and M. Velez, "Enhanced DFT-based channel estimation for LDM systems over SFN channels," in *Proceedings IEEE International Symposium on Broadband Multimedia Systems and Broadcasting*, Ghent, Belgium, June 2015.

[12] *Implementation Guidelines for a Second Generation Digital Terrestrial Television Broadcasting System*, ETSI Std. TS 102 831 V1.2.1, Aug 2012.